MDPI

Short Note

(2*R*, 4*S*, 5*S*) 1-(4-(4-(((7-Chloroquinolin-4-yl)amino)methyl)-1*H*-1,2,3-triazol-1-yl)-5-(hydroxymethyl)tetrahydrofuran-2-yl)-5-methylpyrimidine-2,4(1*H*,3*H*)-dione

Houin Kuan [1,†], **Yuhan Xie** [1,†], **Yuzhu Guo** [1], **Alessandra Gianoncelli** [2], **Giovanni Ribaudo** [2,*]
and Paolo Coghi [1,*]

1   School of Pharmacy, Macau University of Science and Technology, Macau 999078, China;
    1909853apa11008@student.must.edu.mo (H.K.); 19098533pa11002@student.must.edu.mo (Y.X.);
    2009853tpa11001@student.must.edu.mo (Y.G.)
2   Department of Molecular and Translational Medicine, University of Brescia, 25213 Brescia, Italy;
    alessandra.gianoncelli@unibs.it
*   Correspondence: giovanni.ribaudo@unibs.it (G.R.); coghips@must.edu.mo (P.C.); Tel.: +853-68145596 (P.C.)
†   These authors contributed equally to this work.

Abstract: 1,2,3-triazole pharmacophore is a widely recognized motif used for a variety of applications, including drug discovery, chemical biology, and materials science. We herein report the synthesis of a derivative of azidothymidine (AZT), which was combined with the 7-chloro quinoline scaffold through a 1,4-disubstituted 1,2,3-triazole. The chemical structure of the new molecule was fully characterized by Fourier transform infrared (FTIR) spectroscopy, proton nuclear magnetic resonance (^{1}H-NMR), carbon-13 nuclear magnetic resonance (^{13}C-NMR), heteronuclear single quantum coherence (HSQC), heteronuclear multiple bond correlation (HMBC) distortionless enhancement by polarization transfer (DEPT), correlation spectroscopy (^{1}H-^{1}H-COSY), ultraviolet (UV) spectroscopy, and high-resolution mass spectrometry (HRMS). Computational studies were used to predict the interaction of the synthesized compound with HIV reverse transcriptase, a target of relevance for developing new therapeutics against AIDS. The drug-likeness of the compound was also investigated by computing the physico-chemical properties that are important for the pharmacokinetic profile.

Keywords: HIV; 1,2,3-triazole; drug discovery; molecular docking

1. Introduction

Human immunodeficiency virus type 1 (HIV-1) is a retrovirus that is responsible for acquired immune deficiency syndrome (AIDS), which is one of major global public health issues.

In 2021, it was estimated that there were 38.4 million people living with HIV and that 650,000 people died from HIV-related causes [1].

Among the available therapeutic approaches, azidothymidine (AZT, **1,** Figure 1) was the first nucleoside antiviral to be approved for the treatment and prevention of HIV/AIDS [2,3] and it is an inhibitor of the reverse transcriptase (NRTI) enzyme that catalyzes the transcription of retroviral RNA into DNA.

Typically, the inhibitors from this class lack the 3′-OH and act as chain terminators of viral DNA; similarly, the 3′-azido group of AZT can contribute to HIV reverse transcriptase binding and inhibition.

Modifying the 3′-azido group of AZT could yield novel classes of NRTIs and the derivatization by Cu(I)-catalyzed 1,3-dipolar azide-alkyne cycloaddition (click chemistry, CuAAC) to form 1,2,3-triazoles represents an example.

In fact, it has been reported that 1,2,3-triazole and its derivatives have the potential to block a number of HIV-1 enzymes such as reverse transcriptase, integrase, and protease,

and thus this scaffold can be used as a framework for developing new potential anti-HIV-1 agents [4].

In general, triazole hybrids display a range of biological activities, such as antibacterial [5], antitubercular [6], antiviral [7], antimalarial, and anti-inflammatory effects. This has led to significant interest in developing novel compounds based on the 1,2,3-triazole scaffold with potential therapeutic applications.

Previously, we have reported the synthesis of novel 7-chloro quinoline-based 1,2,3-triazole hybrids [8,9] that were also studied for their potential use against SARS-CoV-2 [10].

Boelaert et al. reported an additive effect on HIV when the antimalarial compound chloroquine (CQ, Figure 1) was administered in combination with AZT [11]. Additionally, people affected by AIDS are more likely to experience frequent attacks of malaria, necessitating a combination of antiretroviral therapy and antimalarial medications [12].

This study describes the synthesis and computational studies of a 7-chloro quinoline derivative in which the scaffold has been linked to AZT via a 1,2,3-triazole ring.
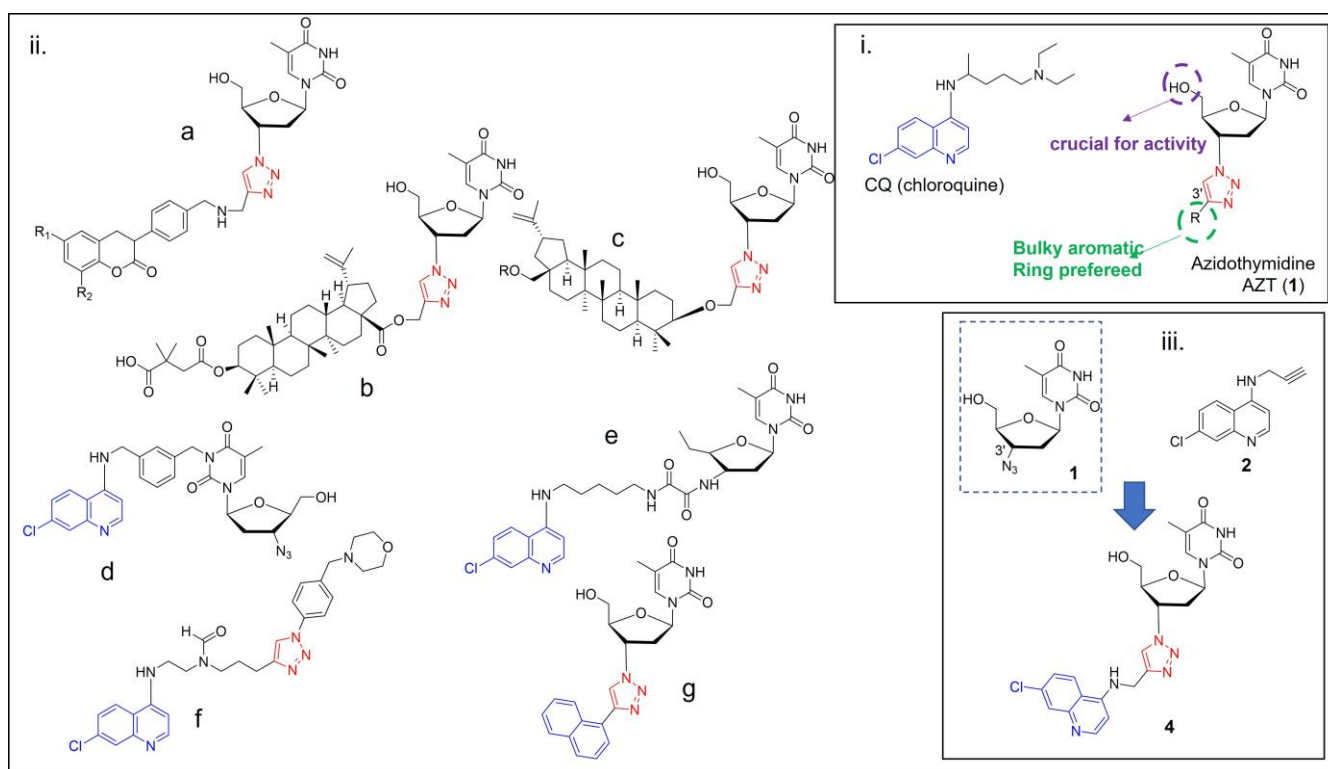

Figure 1. (**i**) Functional groups that are important for the antiviral activity in AZT and the structure of chloroquine (CQ). (**ii**) Examples of 1,2,3-triazole (red) AZT derivatives reported in the literature (**a**–**c**) [13,14] and 1,2,3 triazole/AZT-containing quinoline/aromatic ring (blue) compounds active against retroviruses (**d**–**g**) [7,14–16]. (**iii**) Representative synthetic scheme for obtaining compound **4**, the object of the present work.

2. Results and Discussion

The synthetic route for the triazole hybrid compound, (2*R*, 4*S*, 5*S*) 1-(4-(4-(((7-chloroquinolin-4-yl)amino)methyl)-1*H*-1,2,3-triazol-1-yl)-5-(hydroxymethyl)tetrahydrofuran-2-yl)-5-methylpyrimidine-2,4(1*H*,3*H*)-dione **4**, started from the preparation of the precursor *N*-(Prop-2-yn-1-yl)-7-chloroquinolin-4-amine 3 (Scheme 1a).
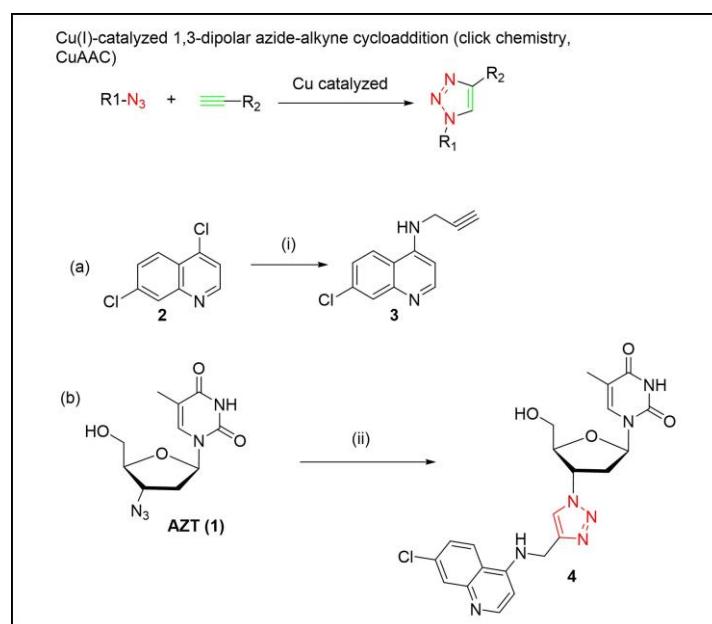
Scheme 1. Synthesis of 1-(4-(4-(((7-chloroquinolin-4-yl)amino)methyl)-1*H*-1,2,3-triazol-1-yl)-5-(hydroxymethyl)tetrahydrofuran-2-yl)-5-methylpyrimidine-2,4(1*H*,3*H*)-dione **4**; (i) propargylamine, N$_2$; (ii) **3**, CuSO$_4$, sodium ascorbate, *t*BuOH/water (1:1). The preparation of intermediate **3** is depicted in (**a**), and of compound **4** in (**b**).

Similar to the protocol reported in the literature [17], quinoline 3 was prepared by the reaction of 4,7-dichloroquinoline **2** with propargyl amine (two equivalents), heating the mixture for 17 h at 110 °C (Scheme 1a). The crude product was purified by recrystallization from EtOAc/hexane to afford 3 in 73% yield.

Propynyl-functionalized derivative **3** was used as a starting compound in the CuAAC cycloaddition by using a modified protocol of the click reaction reported by Feldman et al. [18]. Equimolar amounts of quinoline **3** and AZT in *t*BuOH/water (1:1) were subjected to sequential additions of sodium ascorbate (0.4 equiv.) and CuSO$_4$ (20 mol%) (Scheme 1b). After stirring at 65 °C for 24 h, compound **4** was isolated by column chromatography in a high yield (73%).

The chemical structure of compound **4** was confirmed by NMR, IR, and HRMS analyses, as discussed in the following.

The ^{1}H-NMR spectrum showed a singlet at 4.62 ppm associated with the C9-methylene group and a singlet at 8.24 ppm associated with the position of the C11. Regarding the ^{13}C-NMR signals, the disappearance of the characteristic peaks of the acetylenic group at 74.2 and 80.9 ppm and the appearance of a C-13 methylene signal at 38.1 ppm and a C-11 vinylic signal at 123.8 ppm were probably the most relevant features to verify the incorporation of a triazole moiety.

Heteronuclear single quantum coherence spectroscopy (HSQC), correlation spectroscopy (^{1}H-^{1}H-COSY), and distortionless enhancement by polarization transfer (DEPT-135, DEPT-90, and DEPT-45) were also used to assign ^{13}C signals of compound **4,** as shown in Table S1 (see Supplementary Material for 2D spectra, Figures S7–S11). The ^{13}C-NMR spectrum of **4** exhibited 22 carbon signals, classified by DEPT experiments as one methyl group and three methylene, five methine, five aromatic, and eight quaternary carbons.

In addition, through the observed correlations in the HMBC spectrum of **4**, we were able to unequivocally assign all non-protonated carbons (Figure S12).

The HRMS and UV spectra of **4** were also recorded for further characterization (Supplementary Materials, Figures S13 and S14).

The UV spectrum of compound **4** showed an absorption peak at 250–270 nm and another absorption peak at 320–350 nm (n→π transition) in water and acetone (Supple-

mentary Material, Figure S14a,b). In acetone, it was possible observe two distinct bands sensitive to the monomer–dimer balance (Figure S14b).

The IR spectrum of compound **4** showed characteristic N–H stretching at 3332 cm^{-1}, C=O stretching of lactam at 1662 cm^{-1}, and C=C stretching at 1612 cm^{-1} (Supplementary Materials, Figure S15a). Other vibrational peaks at 1535 and 1435 cm^{-1} were detected, corresponding to the N–H bending in the amide. Moreover, the absence of the N=N=N azide stretching peak of **1** at 2113 cm^{-1} in the IR spectrum of **4** confirmed the conversion of the azide to the triazole (Supplementary Materials, Figure S15a,b).

In order to investigate whether compound **4** could be a good candidate as a reverse transcriptase inhibitor, we performed molecular modeling studies. Thus, molecular docking was enrolled to preliminarily investigate the interaction of the molecule with this target. In particular, the crystal structure of HIV-1 reverse transcriptase in a complex with DNA and AZT was used (PDB ID 3V4I) [19]. Site-specific docking was performed, and the accuracy of the method was checked by re-docking the cognate ligand, which was superimposed to the original pose (-9.6 kcal/mol).

The mechanism of inhibition requires subsequent phosphorylations by cellular kinases [20]; thus, to allow a fair comparison of the interaction motif, compound **4** was modified to its phosphorylated form during docking preparation.

Compound **4** fitted within the identified binding pocket, partially sharing a similar interaction motif (Figure 2). In particular, the ligands showed a good co-localization of phosphate groups, which are in close proximity to the magnesium ion. In Figure 2, the residues within interaction distance (<5 Å) have been labelled.
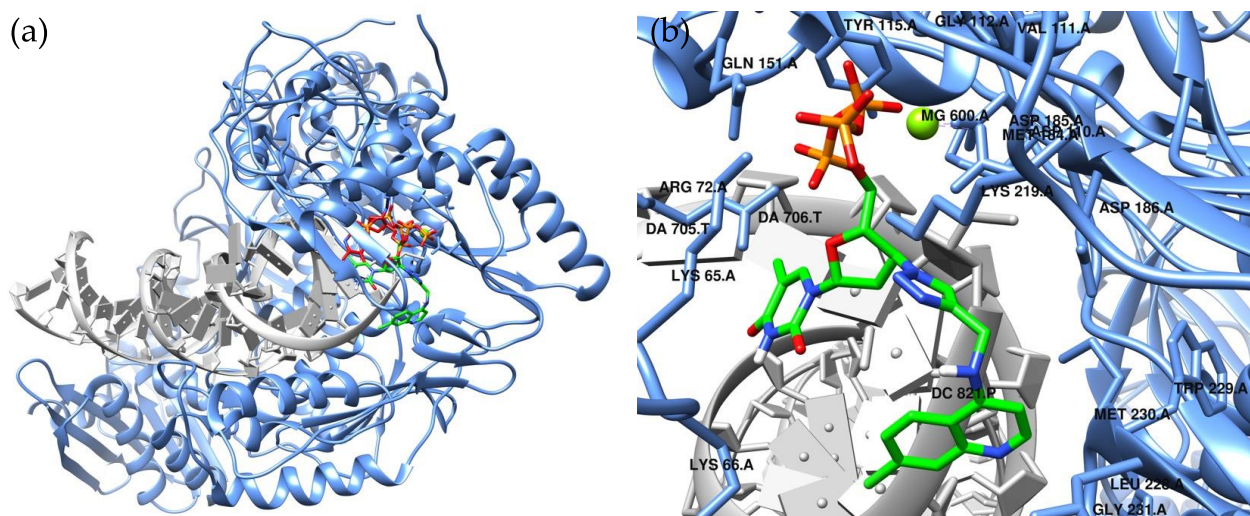

Figure 2. Three-dimensional structure of HIV-1 reverse transcriptase in complex with DNA and **1**, which is depicted in red (PDB ID 3V4I). The computed binding pose for compound **4** is represented in green (**a**). A magnification of the binding site is shown in panel (**b**), showing the interaction motif predicted for compound **4**.

Thus, compound **4** fits in an appropriate way into the binding site, and a promising calculated binding energy value (-11.6 kcal/mol), which exceeds the one obtained from the re-docking of AZT, was computed for this molecule.

Compound **4** was evaluated for its physicochemical properties and oral bioavailability by using predictive modeling. The results of these calculations (see Supplementary Materials, Table S2) showed that compound **4** adhered to all of Lipinski's rules, suggesting that it possesses drug-like properties. This finding corroborates the results of the gastrointestinal absorption model from SwissADME, in which compound **4** was predicted to be highly absorbed according to a BOILED-Egg graph (Figure S16) [21].

3. Materials and Methods

3.1. Chemistry

Silica gel (FCP 230–400 mesh) was used for column chromatography. Thin-layer chromatography was carried out on E. Merck precoated silica gel 60 F$_{254}$ plates and visualized with phosphomolybdic acid, iodine, or a UV–visible lamp.

All chemicals were purchased from Bide Pharmatech., Ltd. (Shanghai, China) and J & K scientific (Hong Kong, China). ^{1}H-NMR and ^{13}C-NMR spectra were collected in CDCl$_3$ at 25 °C on a Bruker Ascend®-600 NMR spectrometer (Bruker, Billerica, MA, USA (600 MHz for ^{1}H and 150 MHz for ^{13}C). All chemical shifts were reported in the standard δ notation of parts per million using the peak of residual proton signals of CDCl$_3$ or DMSO-d6 as an internal reference (CDCl$_3$, δ$_C$ 77.2 ppm, δ$_H$ 7.26 ppm; DMSO-d6, δ$_C$ 39.5 ppm, δ$_H$ 2.50 ppm). High-resolution mass spectra (HRMS) were measured using electrospray ionization (ESI). The measurements were performed in positive ion mode (interface capillary voltage 4500 V), the mass ratio was from *m/z* 50 to 3000 Da, and external/internal calibration was performed with Electrospray Calibration Solution.

HRMS analyses were performed by an Agilent 6230 electrospray ionization (ESI) time-of-flight (TOF) mass spectrometer (Santa Clara, CA, USA) with an Agilent C18 column (4.6 mm × 150 mm, 3.5 μm). The mobile phase was isocratic (water + 0.01% TFA; CH$_3$CN) at a flow rate of 0.35 mL/min.

The UV analysis was performed by a Shimadzu UV–2600 (Osaka, Japan) with a 1 cm quartz cell and a slit width of 2.0 nm. The analysis was carried out using wavelengths in the range of 200–450 nm.

The FT-IR analysis was performed by a Shimadzu IRAffinity-1S (Osaka, Japan) with a frequency range of 4000–500 cm^{-1} with a SPECAC ATR accessory.

3.1.1. Synthesis of *N*-(Prop-2-yn-1-yl)-7-chloroquinolin-4-amine (**3**)

The spectral characteristics are consistent with those of **3** in the literature [17].

Yield 63%, m.p. 158 °C (dec.) δ$_H$ (600 MHz, DMSO-*d6*) 3.19 (1H, *J* = 2.4 Hz, t, C*H*), 4.14 (2H, *J* = 5.7 and 2.4 Hz, dd, C*H*2), 6.61 (1H, *J* = 5.4 Hz, d, H–3), 7.48 (1H, *J* = 8.9 and 2.2 Hz, dd, H–6), 7.77 (1H, *J* = 5.7 Hz, t, NH), 7.84 (1H, *J* = 2.2 Hz, d, H–8), 8.20 (1H, *J* = 9.1 Hz, d, H–5), 8.49 (1H, d, *J* = 5.3 Hz, H–2) ppm; δ$_C$ (150MHz, CDCl$_3$) 32 (NHCH2), 74.2 (C alkyne), 80.9 (C alkyne), 100.3 (C3), 118.0, 124.3 (C5), 125.0 (C6), 128.1 (C8), 133.9, 149.4, 149.9, 152.3 (C2) ppm. HRMS-ESI *m/z* 217.0528 [M + H]$^+$ (calcd. for C$_{12}$H$_{10}$ClN$_2$, *m/z* 217.0527)

3.1.2. Synthesis of 1-(4-(4-(((7-Chloroquinolin-4-yl)amino)methyl)-1*H*-1,2,3-triazol-1-yl)-5-(hydroxymethyl)tetrahydrofuran-2-yl)-5-methylpyrimidine-2,4(1*H*,3*H*)-dione (**4**)

The N-propargyl derivative 3 (1 mmol) and azide **1** were dissolved in 5 mL *t*BuOH/water (1:1) and, while stirring at 65 °C, 1 M sodium ascorbate (0.4 mL, 0.4 mmol) and 1 M CuSO$_4$ (0.2 mL, 20 mol%) were added sequentially, in that order. The reaction mixture was then stirred at 65 °C for 24 h. The crude product was then precipitated out by slowly adding cold water to the reaction mixture, after which it was filtered, washed with water, air dried, and purified by silica column chromatography (eluents: from CH$_2$Cl$_2$ to 5% MeOH). Yield 73%, δ$_H$ (600 MHz, DMSO-*d6*) 1.78 (3H, s, CH3), 2.61–2.71 (2H, m, H–13), 3.57–3.67 (2H, m, H–16), 4.19 (1H, m, H–15), 4.62 (2H, d, *J* = 5.6 Hz, H–9), 5.25 (1H, t, OH), 5.33 (1H, m, H–12), 6.40 (1H, *J* = 6.6 Hz, t, H –14), 6.62 (1H, *J* = 5.5 Hz, d, H–3), 7.49 (1H, dd, *J* = 9 and 2.2 Hz, H -6), 7.79 (1H, *J* = 2.2 Hz, d, H–20), 7.82 (1H, d, *J* = 2.2 Hz, H–8), 8.08 (br, NH), 8.24 (1H, s, H–11), 8.29 (1H, d, *J* = 9.1 Hz, H–5), 8.42 (1H, d, *J* = 5.5 Hz, H–2), 11.34 (1H, s, NH) ppm; δ$_C$ (150 MHz, CDCl$_3$) 13.2 (CH3), 38.1 (C-13), 38.9 (C-9), 60.1 (C-12), 61.7 (C-16), 84.8 (C-14), 85.4 (C-15), 100.2 (C-3), 110.6, 118.5, 123.8 (C-11), 125.1 (C-6), 125.5 (C-5), 127.8 (C-8), 134.8, 137.2 (C-20), 145.4, 149.2, 151.1, 151.4 (C-17), 152.1 (C-2), 164.8 (C-18) ppm; HRMS-ESI *m/z* 484.1518 [M + H]$^+$ (calcd. for C$_{22}$H$_{22}$ClN$_7$O$_4$, *m/z* 484.1495); UV (acetone) peaks 270 and 330 nm, (water) peaks 256 and 326, 339 nm.

3.2. Computational Studies

The 3D X-ray crystal structure of HIV-1 reverse transcriptase in complex with DNA and AZT was retrieved from the RCSB Protein Data Bank (www.rcsb.org, PDB ID 3V4I, resolution 2.80 Å) (accessed on 19 May 2023) [19].

Prior to site-specific docking studies, the protein was prepared and selected chains were isolated and considered. The ligand was built and modified to its phosphorylated form using Avogadro [22]. The site-specific molecular docking study was performed using AutoDock Vina [22,23]. The search volume was centered on the cognate ligand and set according to the following parameters: x = 9.8614, y = 25.659, z = 38.850; size: 20.000 × 20.000 × 20.000 Å. The docking simulation was carried out with default Vina parameters, the number of generated docking poses was set to 8 and docking energy conformation value was expressed in -kcal/mol. The best scoring pose was selected for further analyses.

UCSF Chimera molecular viewer was used to produce the artworks [24]. The ADME properties for compound **4** were retrieved using the SwissADME tool.

4. Conclusions

In conclusion, we synthesized a new hydro-soluble AZT derivative by employing a click chemistry approach. The product was obtained with a good yield and fully characterized by NMR, IR, UV, and HRMS analyses. Compound **4**, which has been shown to be a good candidate for the inhibitory action of reverse transcriptase according to computational site-specific molecular docking experiments, also showed good predicted physico-chemical properties, suggesting that the derivative is a drug-like molecule. Thus, compound **4** represents a promising starting point for in vitro testing and further optimization.

Supplementary Materials: The following supporting information are available online, Figure S1: 1H NMR of compound **3**, Figure S2: 13C NMR of compound **3**, Figure S3: 1H NMR of compound **1**, Figure S4: 13C NMR of compound **1**, Figures S5 and S6: 1H and 13C of compound **4**, Figure S7a: HSQC spectra of **4**, Figure S8a: 1H-1H COSY of **4**, Figures S9–S11: DEPT spectrum of **4**, Figure S12 HMBC of **4**, Figure S13: HR-MS of **4**, Figure S14a: UV spectrum of **4** in acetone, Figure S14b: UV spectrum of **4** in water, Figure S15a: IR spectrum of compound **4**, Figure S15b: IR spectrum of compound **1**, Table S1: 1H- and 13C-nuclear magnetic spectroscopy (NMR) chemical shifts, Table S2: physicochemical properties of **4** calculated by SwissADME, Figure S16: BOILED-Egg graph, [21,25,26].

Author Contributions: Conceptualization, P.C.; methodology, Y.X., H.K. and Y.G.; software, H.K.; validation, P.C.; formal analysis, Y.X.; investigation, Y.X. and H.K.; data curation, Y.X. and H.K.; writing—original draft preparation, Y.X. and H.K.; writing—review and editing, A.G., G.R. and P.C.; supervision, P.C.; project administration, P.C.; funding acquisition, P.C. All authors have read and agreed to the published version of the manuscript.

Data Availability Statement: Not applicable.

Sample Availability: Samples of the compounds are available from the authors.

References

1. World Health Organization. Available online: https://www.who.int/news-room/fact-sheets/details/hiv-aids (accessed on 30 May 2023).
2. Broder, S. The development of antiretroviral therapy and its impact on the HIV-1/AIDS pandemic. *Antivir. Res.* **2010**, *85*, 1–18. [CrossRef]
3. Wright, K. AIDS therapy. First tentative signs of therapeutic promise. *Nature* **1986**, *323*, 283. [CrossRef]
4. Feng, L.S.; Zheng, M.J.; Zhao, F.; Liu, D. 1,2,3-Triazole hybrids with anti-HIV-1 activity. *Arch. der Pharm.* **2021**, *354*, e2000163. [CrossRef]
5. Demaray, J.A.; Thuener, J.E.; Dawson, M.N.; Sucheck, S.J. Synthesis of triazole-oxazolidinones via a one-pot reaction and evaluation of their antimicrobial activity. *Bioorganic Med. Chem. Lett.* **2008**, *18*, 4868–4871. [CrossRef] [PubMed]

6. Tripathi, R.P.; Yadav, A.K.; Ajay, A.; Bisht, S.S.; Chaturvedi, V.; Sinha, S.K. Application of Huisgen (3+2) cycloaddition reaction: Synthesis of 1-(2,3-dihydrobenzofuran-2-yl-methyl [1,2,3]-triazoles and their antitubercular evaluations. *Eur. J. Med. Chem.* **2010**, *45*, 142–148. [CrossRef]

7. Herrmann, L.; Hahn, F.; Wangen, C.; Marschall, M.; Tsogoeva, S.B. Anti-SARS-CoV-2 Inhibitory Profile of New Quinoline Compounds in Cell Culture-Based Infection Models. *Chem. Eur. J.* **2022**, *28*, e202103861. [CrossRef] [PubMed]

8. Fai, L.K.; Anyanwu, M.; Ai, J.; Xie, Y.; Gianoncelli, A.; Ribaudo, G.; Coghi, P. 4-(4-(((1*H*-Benzo[d][1,2,3]triazol-1-yl)oxy)methyl)-1*H*-1,2,3-triazol-1-yl)-7-chloroquinoline. *Molbank* **2022**, *2022*, M1404. [CrossRef]

9. Coghi, P.; Ng, J.P.L.; Nasim, A.A.; Wong, V.K.W. *N*-[7-Chloro-4-[4-(phenoxymethyl)-1*H*-1,2,3-triazol-1-yl]quinoline]-acetamide. *Molbank* **2021**, *2021*, M1213. [CrossRef]

10. Yun, X.; Xie, Y.; Ng, J.P.L.; Law, B.Y.K.; Wong, V.K.W.; Coghi, P. 2-Bromo-3-((1-(7-chloroquinolin-4-yl)-1*H*-1,2,3-triazol-4-yl)-methoxy)-benzaldehyde. *Molbank* **2022**, *2022*, M1351. [CrossRef]

11. Boelaert, J.R.; Sperber, K.; Piette, J. The additive in vitro anti-HIV-1 effect of chloroquine, when combined with zidovudine and hydroxyurea. *Biochem. Pharmacol.* **2001**, *61*, 1531–1535. [CrossRef]

12. Fehintola, F.A.; Akinyinka, O.O.; Adewole, I.F.; Maponga, C.C.; Ma, Q.; Morse, G.D. Drug interactions in the treatment and chemoprophylaxis of malaria in HIV infected individuals in sub Saharan Africa. *Curr. Drug Metab.* **2011**, *12*, 51–56. [CrossRef]

13. Bori, I.D.; Hung, H.Y.; Qian, K.; Chen, C.H.; Morris-Natschke, S.L.; Lee, K.H. Anti-AIDS agents 88. Anti-HIV conjugates of betulin and betulinic acid with AZT prepared via click chemistry. *Tetrahedron Lett.* **2012**, *53*, 1987–1989. [CrossRef] [PubMed]

14. Sirivolu, V.R.; Vernekar, S.K.; Ilina, T.; Myshakina, N.S.; Parniak, M.A.; Wang, Z. Clicking 3'-azidothymidine into novel potent inhibitors of human immunodeficiency virus. *J. Med. Chem.* **2013**, *56*, 8765–8780. [CrossRef] [PubMed]

15. Ivasiv, V.; Albertini, C.; Gonçalves, A.E.; Rossi, M.; Bolognesi, M.L. Molecular Hybridization as a Tool for Designing Multitarget Drug Candidates for Complex Diseases. *Curr. Top. Med. Chem.* **2019**, *19*, 1694–1711. [CrossRef]

16. Aminake, M.N.; Mahajan, A.; Kumar, V.; Hans, R.; Wiesner, L.; Taylor, D.; de Kock, C.; Grobler, A.; Smith, P.J.; Kirschner, M.; et al. Synthesis and evaluation of hybrid drugs for a potential HIV/AIDS-malaria combination therapy. *Bioorganic Med. Chem.* **2012**, *20*, 5277–5289. [CrossRef] [PubMed]

17. Fisher, G.M.; Tanpure, R.P.; Douchez, A.; Andrews, K.T.; Poulsen, S.A. Synthesis and evaluation of antimalarial properties of novel 4-aminoquinoline hybrid compounds. *Chem. Biol. Drug Des.* **2014**, *84*, 462–472. [CrossRef]

18. Feldman, A.K.; Colasson, B.; Fokin, V.V. One-pot synthesis of 1,4-disubstituted 1,2,3-triazoles from in situ generated azides. *Org. Lett.* **2004**, *6*, 3897–3899. [CrossRef]

19. Santos, L.H.; Ferreira, R.S.; Caffarena, E.R. Computational drug design strategies applied to the modelling of human immunodeficiency virus-1 reverse transcriptase inhibitors. *Mem. do Inst. Oswaldo Cruz* **2015**, *110*, 847–864. [CrossRef]

20. Furman, P.A.; Fyfe, J.A.; St Clair, M.H.; Weinhold, K.; Rideout, J.L.; Freeman, G.A.; Lehrman, S.N.; Bolognesi, D.P.; Broder, S.; Mitsuya, H. Phosphorylation of 3'-azido-3'-deoxythymidine and selective interaction of the 5'-triphosphate with human immunodeficiency virus reverse transcriptase. *Proc. Natl. Acad. Sci. USA* **1986**, *83*, 8333–8337. [CrossRef]

21. Daina, A.; Michielin, O.; Zoete, V. SwissADME: A free web tool to evaluate pharmacokinetics, drug-likeness and medicinal chemistry friendliness of small molecules. *Sci. Rep.* **2017**, *7*, 42717. [CrossRef]

22. Hanwell, M.D.; Curtis, D.E.; Lonie, D.C.; Vandermeersch, T.; Zurek, E.; Hutchison, G.R. Avogadro: An advanced semantic chemical editor, visualization, and analysis platform. *J. Cheminformatics* **2012**, *4*, 17. [CrossRef] [PubMed]

23. Trott, O.; Olson, A.J. AutoDock Vina: Improving the speed and accuracy of docking with a new scoring function, efficient optimization, and multithreading. *J. Comput. Chem.* **2010**, *31*, 455–461. [CrossRef] [PubMed]

24. Pettersen, E.F.; Goddard, T.D.; Huang, C.C.; Couch, G.S.; Greenblatt, D.M.; Meng, E.C.; Ferrin, T.E. UCSF Chimera--a visualization system for exploratory research and analysis. *J. Comput. Chem.* **2004**, *25*, 1605–1612. [CrossRef] [PubMed]

25. Adasme, M.F.; Linnemann, K.L.; Bolz, S.N.; Kaiser, F.; Salentin, S.; Haupt, V.J.; Schroeder, M. PLIP 2021: Expanding the Scope of the Protein–Ligand Interaction Profiler to DNA and RNA. *Nucleic Acids Research* **2021**, *49*, W530–W534. [CrossRef] [PubMed]

26. Daina, A.; Zoete, V. A BOILED-Egg To Predict Gastrointestinal Absorption and Brain Penetration of Small Molecules. *ChemMedChem* **2016**, *11*, 1117–1121. [CrossRef] [PubMed]